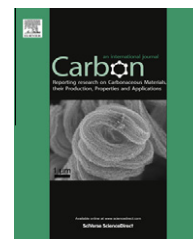


Available at [www.sciencedirect.com](http://www.sciencedirect.com)

SciVerse ScienceDirect

journal homepage: [www.elsevier.com/locate/carbon](http://www.elsevier.com/locate/carbon)

# An increase in the field emission from vertically aligned multiwalled carbon nanotubes caused by NH<sub>3</sub> plasma treatment

Guohai Chen <sup>a</sup>, Suman Neupane <sup>a</sup>, Wenzhi Li <sup>a,\*</sup>, Lina Chen <sup>b</sup>, Jiandi Zhang <sup>b</sup><sup>a</sup> Department of Physics, Florida International University, Miami, FL 33199, USA<sup>b</sup> Department of Physics & Astronomy, Louisiana State University, Baton Rouge, LA 70803, USA

## ARTICLE INFO

### Article history:

Received 6 April 2012

Accepted 26 September 2012

Available online xxxx

## ABSTRACT

We modified vertically aligned multiwalled carbon nanotubes (MWCNTs) grown on a Cu substrate by NH<sub>3</sub> direct current plasma treatment for varying durations and investigated their microstructure and field emission properties. A great improvement on the field emission properties of the MWCNTs was obtained after the plasma treatment. Specifically, the MWCNTs after 1.0 min plasma treatment demonstrated the best field emission performance with the field enhancement factor increasing from 319 to 546, the turn-on electric field decreasing from 11.93 to 8.84 V/μm, and the highest emission current reaching 0.85 mA, as compared to the untreated sample. The improvement was attributed to the morphology change: the tapered structure of the MWCNTs generated by the plasma etching and the increased inter-tip distance due to the cluster structure of the thin tips. The open-ended tips and the increased structural defects introduced by NH<sub>3</sub> plasma also played a role in the enhancement of field emission properties of the MWCNTs.

© 2012 Elsevier Ltd. All rights reserved.

## 1. Introduction

Carbon nanotubes (CNTs) have been considered as the next generation field emission material due to their large aspect ratio, high mechanical stiffness, good electrical conductivity, and excellent thermal and chemical stability [1–3]. Vertically aligned CNTs (VACNTs) demonstrate better field emission performance as compared to randomly oriented CNTs [4,5]. Therefore, many efforts have been focused on growing VACNTs using various methods [6–8]. Field emission properties largely depend on the CNT emitter structure, the CNT species, and especially the CNT morphology, such as the alignment, length, diameter, density and the crystallization of CNTs. Various methods have been developed to improve the field emission performance of CNTs, such as thermal oxidation [4], laser treatment [9], Ar neutral beam treatment [10], ultraviolet laser ablation [11], and plasma treatment [12–19]. Among

these methods, plasma treatment has proven to be an effective and efficient method for enhancing the field emission performance of CNTs by changing the CNT morphology [13], alignment [16], structural defects [20], and work function [19]. Many types of plasma, such as H<sub>2</sub> [12], Ar [13], CF<sub>4</sub> [15], N<sub>2</sub> [16], O<sub>2</sub> [18], and He [21], have been investigated.

In this study, vertically aligned MWCNTs were grown on a Cu substrate by plasma enhanced chemical vapor deposition (PECVD) method. Cu, due to its low catalytic activity, is a commonly used substrate material for the synthesis of graphene by CVD. However, it is still challenging to synthesize well-graphitized VACNTs directly on Cu substrate [22]. We aim to synthesize VACNTs on Cr coated Cu because this allows for the in situ fabrication of electron emitters capable of delivering high current without the post-transfer onto other conducting substrates. We further aim to treat these CNTs with NH<sub>3</sub> direct current (DC) plasma since NH<sub>3</sub> is one of the

\* Corresponding author: Fax: +1 305 348 6700.

E-mail address: [Wenzhi.Li@fiu.edu](mailto:Wenzhi.Li@fiu.edu) (W. Li).

0008-6223/\$ - see front matter © 2012 Elsevier Ltd. All rights reserved.

<http://dx.doi.org/10.1016/j.carbon.2012.09.058>

primary gasses used during the synthesis, and hence, no additional gasses are needed.  $\text{NH}_3$  plasma not only induces structural changes, but it also creates chemical doping sites on CNTs. The effects of plasma treatment on the microstructure and the field emission properties of the MWCNTs were investigated. It was found that the MWCNTs changed from the cylindrical shape to the tapered shape after plasma treatment. The tips of the adjacent MWCNTs could easily touch each other to form clusters of CNTs connected at the tip. The plasma treatment also induced some structural defects into CNTs, created many open-ended tips, and resulted in a nitrogen doping effect. Such features translate into improved MWCNT field emission properties.

## 2. Experimental

MWCNTs were synthesized by PECVD using Ni as a catalyst and Cr as a buffer layer on a Cu substrate. A 15 nm thick Cr layer was deposited on the Cu substrate using e-beam evaporation followed by a 6 nm-thick Ni layer. MWCNTs were synthesized using  $\text{NH}_3/\text{C}_2\text{H}_2$  at 510 °C under a pressure of 8 torr with a plasma power of 80 W for 10 min. The gas flow was maintained at 100 sccm for  $\text{NH}_3$  and 30 sccm for  $\text{C}_2\text{H}_2$ . The plasma treatment was carried out at 510 °C under a pressure of 8 torr with a plasma power of 80 W using  $\text{NH}_3$  flow rate, which was maintained at 100 sccm for 0.5, 1.0 and 2.0 min. The samples were labeled as P-0.0 min, P-0.5 min, P-1.0 min, and P-2.0 min for MWCNTs with plasma treatment for 0, 0.5, 1.0, and 2.0 min, respectively.

The MWCNTs were characterized by scanning electron microscopy (SEM, JEOL JSM-6330F), transmission electron microscopy (TEM, JEOL-2010F), and Raman spectroscopy ( $\text{Ar}^+$  laser excitation, wavelength: 514.5 nm). X-ray photoelectron spectroscopy (XPS) measurements were carried out in an ultra-high vacuum ( $1.0 \times 10^{-10}$  torr) to analyze the possible bonding structure of nitrogen with MWCNTs by probing the N 1s core levels. Field emission measurements were carried out using a planar diode configuration in a vacuum chamber at a pressure level of  $10^{-7}$  torr. The gap between the cathode and the anode was 250  $\mu\text{m}$  and the emission area was 0.785  $\text{cm}^2$ . The emission current was monitored with a Keithley 4200-SCS, and DC power was supplied by a DC power supply (Matsusada AU-15P20).

## 3. Results and discussion

Typical SEM images of the MWCNTs before and after  $\text{NH}_3$  plasma treatment are shown in Fig. 1. The as-synthesized sample P-0.0 min consists of a high-density array of VACNTs, as shown in Fig. 1a. The as-grown CNTs showed a cylindrical structure with a large diameter of around 80 nm. The CNT length was non-uniform and in the range of 1–1.5  $\mu\text{m}$ . Some CNTs were protruding higher than others. These protruding CNTs can act as effective emission sites. After 0.5 min treatment, the MWCNTs became thinner as compared to sample P-0.0 min due to the etching effect of the plasma as shown in Fig. 1b. The plasma treatment also resulted in sharper tips of the MWCNTs as compared with the pristine MWCNTs. In addition, the longer MWCNTs were cut by the plasma, resulting in a relatively uniform length after the plasma etching.

The etching effect became more significant after 1.0 min treatment. As shown in Fig. 1c, the MWCNT showed a tapered structure with a very sharp tip compared with the pristine MWCNTs. This tapered structure is favorable for the field emission because of an increased aspect ratio. The thinner tips also easily touched each other and, as a result, seemed to form a cluster structure. The tips of the MWCNTs form a bundle after 1.0 min treatment as observed in the inset of Fig. 1c. Each bundle consists of several CNTs connected at the tips. Therefore, the inter-tip distance increased for the sample P-1.0 min as compared with the samples P-0.0 min and P-0.5 min, as shown in the insets of Fig. 1a–c. Nilsson et al. predicted that an intertube distance of about 2 times the height of the CNTs optimizes the emitted current per unit area [23]. Recently, Dionne et al. have performed a numerical investigation of the field enhancement factor of individual as well as array of CNTs and confirmed that the spacing between identical CNTs should be about twice their height to minimize the screening effects [24]. In addition, their study also indicated that in an array consisting of CNTs with two different heights, there was no significant screening of the electric field from short CNTs when the taller CNTs were twice the height of the shorter ones. Larger differences in height lead to stronger screening effects on the smaller structures and the smaller CNTs do not contribute significantly to the total field emission current. Therefore, the structure changes after plasma treatment will effectively alleviate the screening effect in the MWCNT film, resulting in the enhanced field emission properties. However, after 2.0 min plasma treatment, the morphology of the MWCNTs was drastically different from the previous samples, as shown in Fig. 1d. The prolonged plasma treatment resulted in a severe damage to the structure and alignment of MWCNTs as shown in the inset of Fig. 1d. Hence, a significant decrease in the field emission performance is expected for the CNTs with the prolonged plasma treatment.

TEM observations were carried out to examine the microstructures of MWCNTs. Fig. 2 shows the TEM images of the MWCNTs before and after  $\text{NH}_3$  plasma treatment. Without the plasma treatment, the MWCNTs showed a cylindrical structure, as shown in Fig. 2a. The crystallinity was not ideal, but graphitic layers could still be found. All the CNTs had closed tips with a catalyst particle at the tip. The MWCNTs had slightly different diameters, which depends on the size of the catalyst fragment produced from the catalyst island. The diameter of the CNTs in Fig. 2a was around 80 nm. The inset in Fig. 2a shows a low magnification TEM image. We found that the MWCNTs showed bamboo-like structures with a catalyst particle trapped at the tip, which is the characteristic of the CNTs synthesized by PECVD process [25]. The graphitic planes in the tube walls are not always parallel to the tube axis but are often twisted and broken, as shown in the inset of Fig. 2a. After 0.5 min treatment, the MWCNTs became thinner due to the plasma etching effect with a diameter of 50 nm, as shown in Fig. 2b. The etching effect was more significant at the tip, resulting in a sharp tip with a diameter of  $\sim 20$  nm. The graphene layers at the tip were particularly damaged, as evidenced by the etched catalyst particles. As a result, the CNTs showed an open tip with some damage on the wall. However, the high resolution TEM image shows a

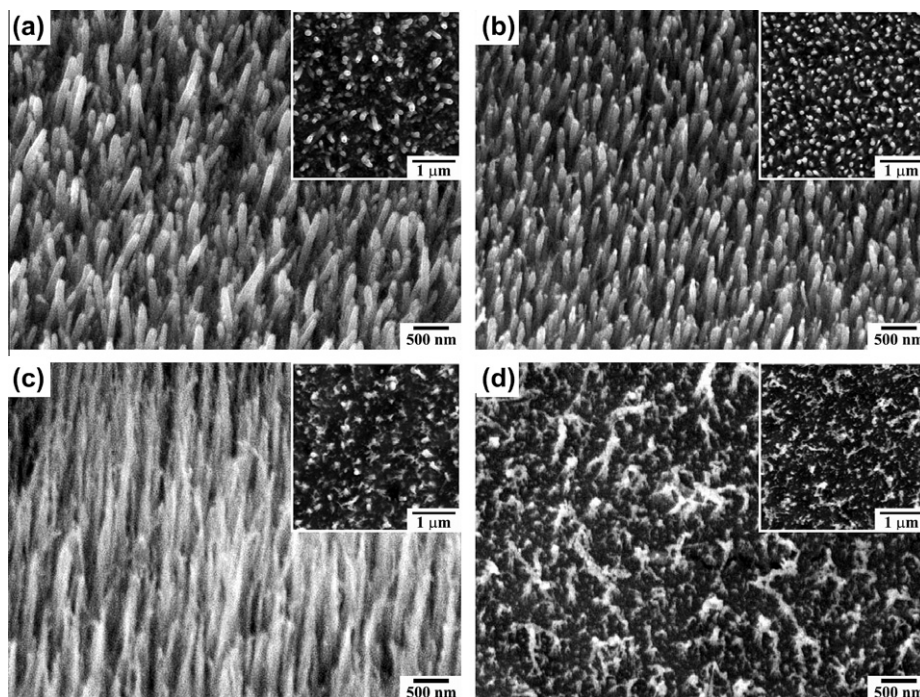


Fig. 1 – SEM images of the MWCNTs before and after  $\text{NH}_3$  plasma treatment: (a) P-0.0 min, (b) P-0.5 min, (c) P-1.0 min, and (d) P-2.0 min. The insets show the corresponding top-view images.

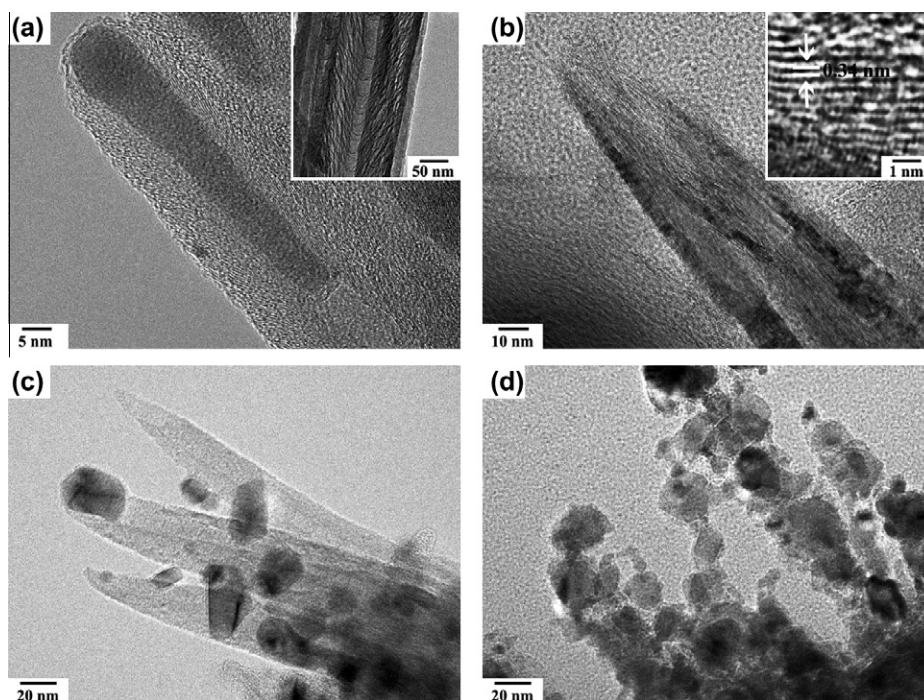


Fig. 2 – TEM images of the MWCNTs before and after  $\text{NH}_3$  plasma treatment: (a) P-0.0 min, (b) P-0.5 min, (c) P-1.0 min, and (d) P-2.0 min. The inset in (a) shows a bamboo-like structure. The inset in (b) shows the lattice fringes of graphitic planes in a single MWCNT.

section of ordered graphitic layers with the separation of about 0.34 nm which corresponds to the separation of lattice planes (0 0 2) of graphite, as shown in the inset of Fig. 2b. The etching effect became more pronounced with continued

plasma treatment, to the extent that the CNTs completely changed from the cylindrical structure to a tapered structure with a very sharp tip, as shown in Fig. 2c. This tapered structure is favorable for field emission due to its large aspect ratio.

After 2.0 min plasma treatment, the MWCNTs were severely destroyed. It was difficult to find the tubular structure under TEM observation, as shown in Fig. 2d. The plasma treatment with longer time induced very severe damage and structural defects to the MWCNTs. Accordingly, the MWCNTs should show greatly degraded field emission performance (more discussions to follow).

Etching effect on various MWCNTs by  $H_2$ ,  $CF_4$ , or  $N_2$  plasma was reported [12,15,16]. Zhu et al. studied  $CF_4$  plasma treatment on cylindrical MWCNTs and similar etching effect was found [15]. Gohel et al. studied morphological changes of MWCNTs treated by  $N_2$  and Ar plasma and found that the nanotube density decreases and the random MWCNTs bundle together to form arrays of vertically aligned nanotube bundles. Each bundle consists of several nanotubes that are joined at their tips [16]. Since our MWCNTs were synthesized by PECVD, they always have amorphous layers and high density of defects on the outside of their walls, they may be easily etched by plasma to form tapered structures than the cylindrical MWCNTs.

To further understand the effect of  $NH_3$  plasma treatment on the field emission properties of MWCNTs, Raman spectroscopy was carried out to analyze the microstructure and defect density of the samples. Raman spectra of the MWCNTs before and after the plasma treatment are shown in Fig. 3a. The graphitic crystal structure of the MWCNTs has a characteristic peak at  $\sim 1593\text{ cm}^{-1}$  (the G band) and a peak at  $\sim 1368\text{ cm}^{-1}$  (the D band). The G band indicates a good arrangement of the hexagonal lattice of graphite (i.e., crystallinity of the sample, pristine arrangement of atoms). The D band gives an indication of defects in CNTs (i.e., carbonaceous impurities with  $sp^3$  bonding, broken  $sp^2$  bonds in the sidewall) [16]. The relative ratio of the intensity of the D band to the G band ( $I_D/I_G$ ) can be considered as the level of the disorder degree in the graphite sheets. Fig. 3b shows the  $I_D/I_G$  ratios for the different plasma treatment time. It can be seen that the  $I_D/I_G$  ratio increased with the plasma treatment time, indicating that the plasma treatment results in some structural defects to the MWCNTs. This is in good agreement with the results of SEM and TEM observations.

The field emission properties of the MWCNTs were investigated. The schematic of the measurement setup is shown in

the upper right inset of Fig. 4a. The anode and cathode were stainless steel plates. The MWCNTs/Cu emitter was attached firmly onto the cathode by applying Ag paste. The Ag paste will also enable a good electrical contact between the cathode and the MWCNTs/Cu emitter during the field emission experiments. Two ceramic plates were used as spacers. For each sample, we repeated the field emission measurement several times to confirm the repeatability of the emission characteristics (emission current versus applied voltage ( $I$ - $V$ ) curves). The MWCNTs demonstrated different field emission properties according to different plasma treatment durations as shown in Fig. 4a. The turn-on electric field ( $E_{\text{turn-on}}$ ) for sample P-0.0 min was  $11.93\text{ V}/\mu\text{m}$ . The  $E_{\text{turn-on}}$  is the field required to obtain an emission current density of  $0.1\ \mu\text{A}/\text{cm}^2$ . After the plasma treatment, the turn-on electric field decreased according to the plasma treatment durations. More specifically, the  $E_{\text{turn-on}}$  for samples P-0.5 min and P-1.0 min were  $10.98$  and  $8.84\text{ V}/\mu\text{m}$ , respectively. However, after 2 min plasma treatment, the  $E_{\text{turn-on}}$  increased slightly to  $10.81\text{ V}/\mu\text{m}$ . The sample P-1.0 min showed the lowest  $E_{\text{turn-on}}$ . In addition, the sample P-1.0 min showed the highest emission current of  $0.85\text{ mA}$ . Both the lowest  $E_{\text{turn-on}}$  and the highest emission current suggest that 1.0 min of  $NH_3$  plasma treatment can greatly improve the field emission performance of MWCNTs.

Several papers calculated the Joule heating effect on CNT during electron emission and reported that the temperature of individual CNT structure can easily go above  $1000\text{ K}$  at an emission current level of  $\mu\text{A}/\text{tube}$  [24,26]. The high temperature might influence the emission regime from a Fowler–Nordheim (F–N) type of emission towards a thermo-field (T–F) emission where tip temperature plays an important role [27–29]. We estimated the current per tube in our research. Considering Fig. 1a as an example, the MWCNT density was estimated to be about  $14\text{ tubes}/\mu\text{m}^2$ . This value was obtained upon considering the screening effect between the MWCNTs with different heights, namely, the short MWCNTs will not contribute significantly to the total field emission current [24]. The maximum emission current density of the P-0.0 min sample was about  $0.18\text{ mA}/\text{cm}^2$ . As a result, the current per tube was around  $1.3 \times 10^{-4}\text{ nA}$ . This value is far below  $300\text{ nA}$ , which is the typical threshold for possible emission degradation of the tubes [30]. We think that high temperatures

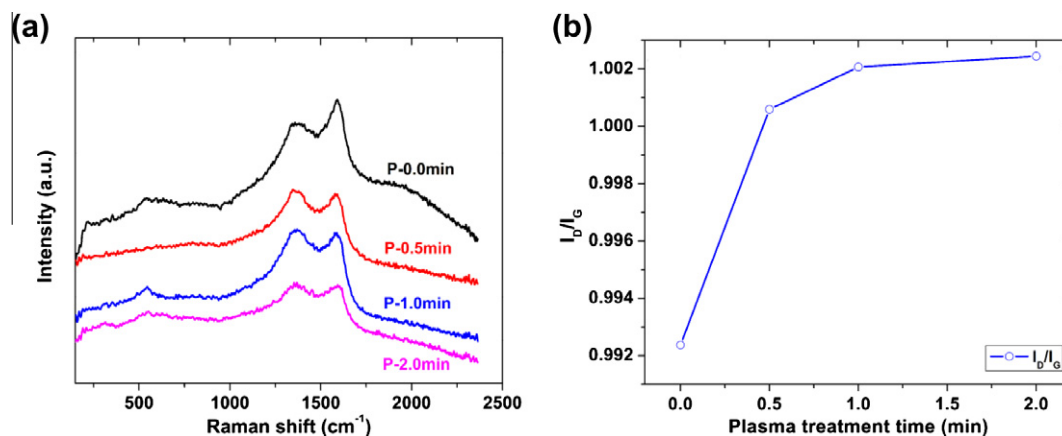
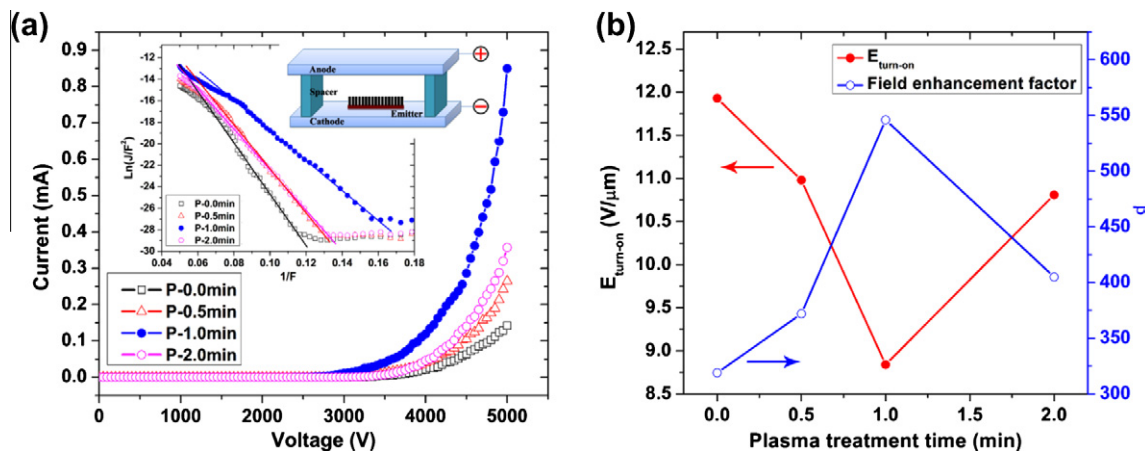


Fig. 3 – (a) Raman spectra of the MWCNTs before and after  $NH_3$  plasma treatment. (b) Corresponding  $I_D/I_G$  ratios.



**Fig. 4** – Field emission characteristics of the MWCNTs before and after  $\text{NH}_3$  plasma treatment. (a)  $I$ – $V$  curves. The inset shows the corresponding  $F$ – $N$  plots and the upper right inset shows the schematic of the field emission measurement setup. (b) Field enhancement factor ( $\beta$ ) and turn-on electric field ( $E_{\text{turn-on}}$ ) of MWCNTs according to  $\text{NH}_3$  plasma treatment time.

on the MWCNT tip might have not been achieved. Therefore, the  $F$ – $N$  equation is still applicable in the present experiment. The inset in Fig. 4a shows the corresponding  $F$ – $N$  plots for the MWCNT emitters. The straight lines indicate the quantum mechanical tunnelling characteristic of field electron emission. The field enhancement factor can be calculated using the  $F$ – $N$  equation:

$$J = A(\beta^2 F^2 / \phi) \exp(-B\phi^{3/2} / \beta F) \quad (1)$$

where  $J$  is the emission current density,  $A = 1.56 \times 10^{-6} \text{ AV}^{-2} \text{ eV}$ ,  $B = 6.83 \times 10^9 \text{ eV}^{-3/2} \text{ Vm}^{-1}$  [31],  $\beta$  is the field enhancement factor,  $\phi$  is the work function, and  $F$  is the applied electric field. Assuming the work function of the MWCNTs to be 5.0 eV [32], the field enhancement factor can be calculated by fitting the slope of the  $F$ – $N$  plot. The field enhancement factors for samples P-0.0 min, P-0.5 min, P-1.0 min, and P-2.0 min were 319, 372, 546, and 405, respectively. We note that the field enhancement factor increased as the plasma treatment time increased, and the MWCNTs with 1 min plasma treatment showed the highest value of the field enhancement factor. Fig. 4b presents the field enhancement factors and  $E_{\text{turn-on}}$  for different plasma treatment time. With the plasma treatment less than 2 min, the field enhancement factor increased and the turn-on electric field decreased, indicating an enhanced field emission performance of the MWCNTs. However, after 2 min plasma treatment, the MWCNTs showed a decreased field enhancement factor and an increased turn-on electric field, indicating that the MWCNTs were damaged severely and showed a degraded field emission performance. Lee et al. studied the field emission characteristics of MWCNTs after Ar plasma treatment and found that the work function slightly increased from 4.57 eV to 4.87 eV (about 6% increase) after 3 min of plasma treatment [19]. If we assume that the work function changed about 6% for samples P-0.0 min and P-1.0 min (i.e. the sample P-0.0 min has a work function of 4.7 eV and the sample P-1.0 min has a work function of 5 eV), the enhancement factor will be 291 for sample P-0.0 min and 546 for sample P-1.0 min corresponding to an increase of 88% in the enhancement factor. In the present work, we use the work function of 5.0 eV for all samples for simplicity. Using the work function of

5.0 eV, the calculated enhancement factor is 319 for sample P-0.0 min and 546 for sample P-1.0 min, corresponding to an increase of 71% in the enhancement factor. Comparing the increase of the enhancement factor (88% and 71%) obtained using different work functions, it is clear that the assumption of the work function of 5.0 eV in this work gave reasonable values for the enhancement factors for samples after different plasma treatment. Fig. 4(b) shows that the enhancement factor increased at first and then decreased as the plasma treatment time increased which was consistent with the results of SEM and TEM observations. Previous studies investigated the relationship between the field enhancement factor, the aspect ratio of CNT structures, and the spacing between CNT structures [24,33]. A more accurate expression for the field enhancement factor was considered as  $\beta = 1.2(2.15 + (h/r))^{0.9}$  [33], with large aspect ratios leading to greater field enhancement factor. Plasma treatment made the CNTs tapered. The tapered CNTs will have increased aspect ratios since their reduced tip diameter can be regarded as the effective diameter. As a result, the field enhancement factor increased. In addition, Dionne et al. concluded that larger field enhancement factor values can be ob-

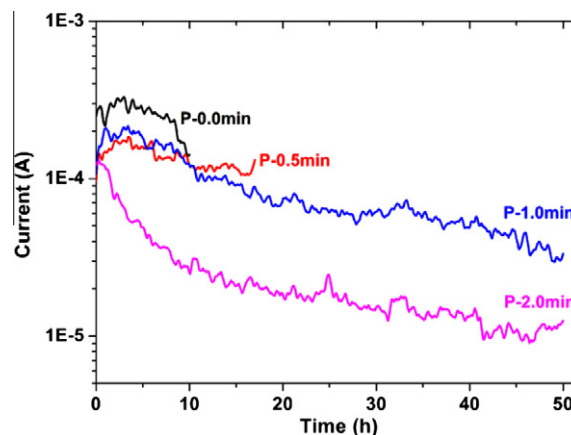


**Fig. 5** – Field emission stability of the MWCNTs before and after  $\text{NH}_3$  plasma treatment.

tained if the spacing between two tubes is greater than the sum of their height ( $\Delta x > h_1 + h_2$ ), whereas significant screening effects will reduce the field enhancement factor if the spacing between the two tubes is equal to or smaller than the sum of their height ( $\Delta x \leq h_1 + h_2$ ) [24]. Therefore, the increased inter-tip distance after plasma treatment resulted in the lowered screening effect and consequently an increased field enhancement factor. It is obvious that the 1 min plasma treatment can greatly improve the field emission performance of the MWCNTs. The tapered CNT structure, the clustered CNT tips, and the increased inter-tip distance due to  $\text{NH}_3$  plasma treatment enhanced the field emission properties of the MWCNTs.

We also evaluated the emission current stability of the MWCNTs before and after  $\text{NH}_3$  plasma treatment as shown in Fig. 5. The initial emission current was around 0.25 mA and then the applied voltage was kept constant for 10 h or longer. The applied voltages were 5000, 4500, 4000, and 4400 V for samples P-0.0 min, P-0.5 min, P-1.0 min, and P-2.0 min, respectively. The initial emission current density was about 0.3 mA/cm<sup>2</sup>, which is a relatively severe condition to visualize current degradation vividly within a relatively short time. Among these MWCNTs, the sample P-1.0 min demonstrated excellent field emission stability over 50 h, even though the emission current still decreased gradually.

The morphology of CNTs can significantly affect their field emission properties. In general, the field enhancement factor is mainly related to the aspect ratio of the CNTs [34]. Its thick diameter and short length may result in a high turn-on electric field due to the small field enhancement factor. After the  $\text{NH}_3$  plasma treatment, the MWCNTs changed from the thick cylindrical structure to the thin tapered structure. As a result, the field enhancement factor increased from 319 to 546 and the turn-on electric field decreased from 11.93 to 8.84 V/ $\mu\text{m}$ . In addition, the tips of the MWCNTs were opened by the plasma treatment, and a high density of structural defects was introduced into the CNTs. CNTs with open-ended tips are favorable for field emission. Both the open-ended tips and structural defects are regarded as one of the possible factors for the improvement on field emission properties of CNTs [12,35]. Moreover, it is well known that the screening effect in the CNT film can significantly reduce the field emission performance of CNTs [23,24]. From the top-view SEM images of the 1.0 min plasma treated sample, the thinner tips of the MWCNTs easily touched each other to form clusters and, as a consequence, the inter-tip distance became a slightly bigger compared with the untreated sample. Therefore, the screening effect will be effectively alleviated.

It is suggested that  $\text{NH}_3$  plasma treatment not only induces structural defects but also creates doping effects. XPS

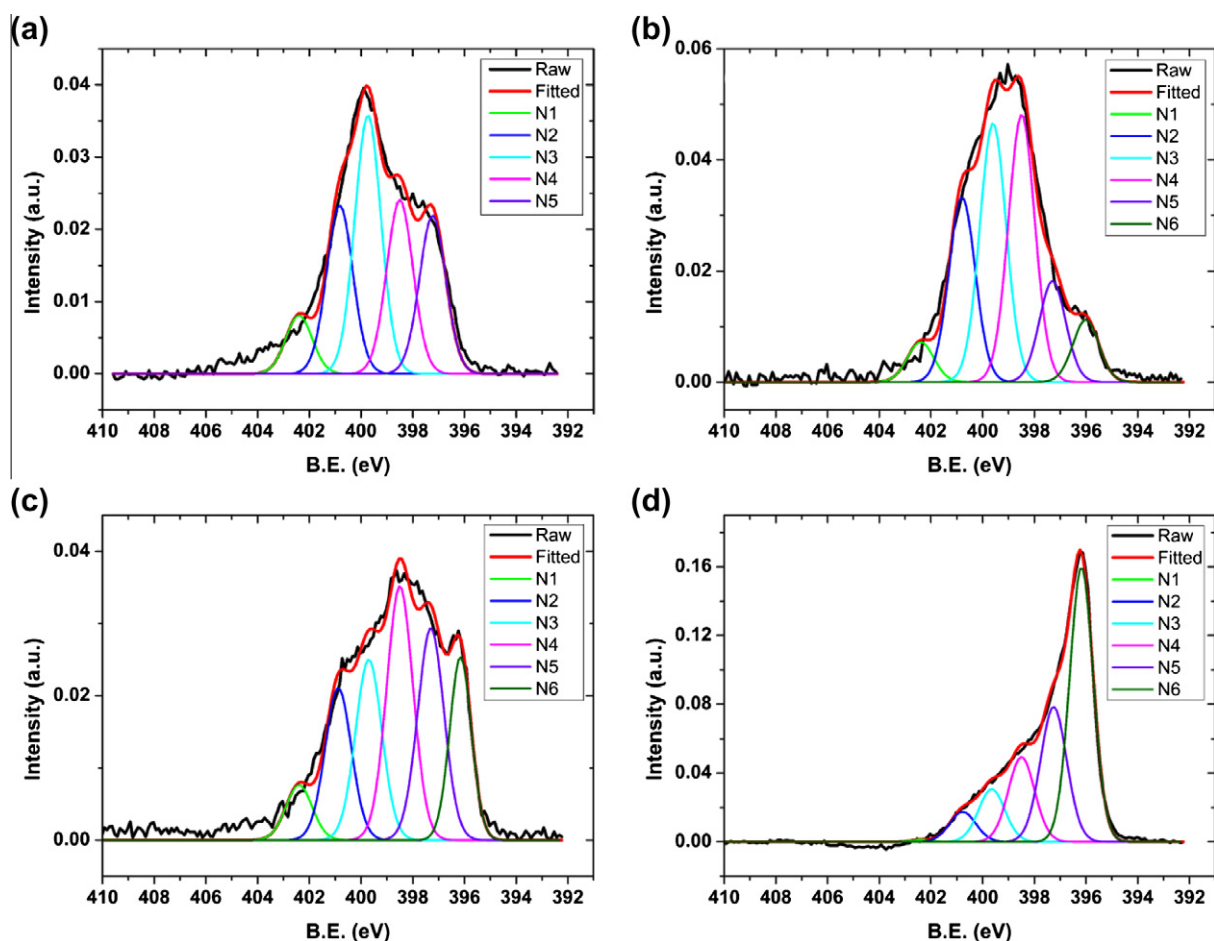


Fig. 6 – XPS spectra from N 1s core level of the MWCNTs before and after  $\text{NH}_3$  plasma treatment: (a) P-0.0 min, (b) P-0.5 min, (c) P-1.0 min, and (d) P-2.0 min.

measurements were carried out to analyze the MWCNTs. The XPS spectra from N 1s core level of the MWCNTs before and after NH<sub>3</sub> plasma treatment are shown in Fig. 6. The spectra can be fitted with component peaks labeled N1, N2, N3, N4, N5, and N6 at 402.5, 400.8, 399.7, 398.6, 397.2, and 396.1 eV, respectively. The values of the full width at half maxima of each peak were about 0.9–1.2 eV, which were in agreement with the previous report [36]. The peaks of N2, N3 and N4 corresponded to NO, C=N (sp<sup>2</sup> bonding), and C≡N (sp<sup>3</sup> bonding), respectively [36]. The high binding energy N1 peak was attributed to interstitial N [16]. The two low binding energy peaks of N5, and N6 were attributed to Cr<sub>2</sub>N [37], and CrN [38], respectively. The intensities of these two peaks increased dramatically, especially after 2 min plasma treatment (not shown here). We can also confirm the chromium nitrides based on the structure change observed under SEM, showing that MWCNTs were badly destroyed so that the substrate was exposed. Considering the growth in this work followed the tip growth mode, many Ni catalyst nanoparticles were encapsulated in the MWCNTs. Therefore, the chromium nitrides formed on the substrate contributed dominantly to the XPS spectra as increasing the plasma treatment time. From the XPS spectra, we have confirmed that nitrogen has been doped into the MWCNTs even for the untreated MWCNTs, since we used NH<sub>3</sub> plasma during growth. Fig. 7 shows the area fraction of CN bonding (N3 and N4 peaks) with respect to the full N 1s spectra for different NH<sub>3</sub> plasma treatment durations. The area fraction reflects the number of CN bonding (N3 and N4 peaks) in the full N 1s spectra. Thus, the number of CN bonding increased at first and then decreased, indicating the doping effect changed along with NH<sub>3</sub> plasma treatment time. The number of CN bonding peaked at 0.5 min NH<sub>3</sub> plasma treatment. Longer the plasma treatment time resulted in lower area fraction of CN bonding. It has been shown that nitrogen doping can improve the field emission performance of CNTs [39,40]. Although 0.5 min NH<sub>3</sub> plasma treatment showed the highest area fraction of CN bonding, NH<sub>3</sub> plasma treatment after 1 min demonstrated the best field emission performance. We suggest that the little difference is mainly attributed to the morphology change. The morphology

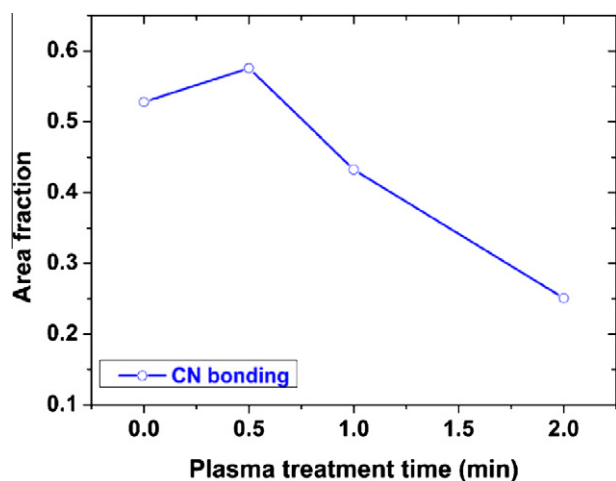


Fig. 7 – Area fraction of CN bonding according to NH<sub>3</sub> plasma treatment time.

change played a dominant role in field emission in this work. Based on the above viewpoints, the NH<sub>3</sub> plasma treatment could greatly improve the field emission performance of the MWCNTs grown on a Cu substrate.

#### 4. Conclusions

The effect of NH<sub>3</sub> plasma treatment on the microstructure and field emission properties of vertically aligned MWCNTs grown on a Cu substrate were investigated. After 1.0 min treatment, a great improvement on the field emission properties of the MWCNTs was obtained. This improvement was caused primarily by the morphology change. The MWCNTs changed from the cylindrical shape to the tapered shape after plasma treatment. The thinner tips of the MWCNTs could easily touch each other to form clusters; consequently, the inter-tip distance increased. The tips of the MWCNTs were opened by the plasma treatment, and a high density of structural defects was introduced into the CNTs, both of which could improve field emission performance. The nitrogen doping induced by NH<sub>3</sub> plasma treatment might also effectively improve the field emission properties. All the results indicate that NH<sub>3</sub> plasma treatment could be an effective way to improve the field emission performance of CNTs.

#### Acknowledgments

This work is supported partially by The American Chemical Society under grant PRF# 51766-ND10 and partially by The National Science Foundation under grant DMR0548061. We are grateful to Dr. Jianyu Huang at Sandia National Laboratories for his help with the TEM examination of the CNTs.

#### REFERENCES

- [1] de Heer WA, Châtelain A, Ugarte D. A carbon nanotube field-emission electron source. *Science* 1995;270(5239):1179–80.
- [2] Saito Y, Uemura S. Field emission from carbon nanotubes and its application to electron sources. *Carbon* 2000;38(2):169–82.
- [3] Sveningsson M, Morian RE, Nerushev O, Campbell EEB. Electron field emission from multi-walled carbon nanotubes. *Carbon* 2004;42(5–6):1165–8.
- [4] Zeng BQ, Xiong GY, Chen S, Wang WZ, Wang DZ, Ren ZF. Enhancement of field emission of aligned carbon nanotubes by thermal oxidation. *Appl Phys Lett* 2006;89(22):223119.
- [5] Chen G, Shin DH, Iwasaki T, Kawarada H, Lee CJ. Enhanced field emission properties of vertically aligned double-walled carbon nanotube arrays. *Nanotechnology* 2008;19(41):415703.
- [6] Li WZ, Xie SS, Qian LX, Chang BH, Zou BS, Zhou WY, et al. Large-scale synthesis of aligned carbon nanotubes. *Science* 1996;274(5293):1701–3.
- [7] Lee CJ, Park J, Kang SY, Lee JH. Growth and field electron emission of vertically aligned multiwalled carbon nanotubes. *Chem Phys Lett* 2000;326(1–2):175–80.
- [8] Hata K, Futaba DN, Mizuno K, Namai T, Yumura M, Iijima S. Water-assisted highly efficient synthesis of impurity-free single-walled carbon nanotubes. *Science* 2004;306(5700):1362–4.
- [9] Chen KF, Chen KC, Jiang YC, Jiang LY, Chang YY, Hsiao MC, et al. Field emission image uniformity improvement by laser

- treating carbon nanotube powders. *Appl Phys Lett* 2006;88(19):193127.
- [10] Kyung SJ, Park JB, Park BJ, Lee JH, Yeom GY. Improvement of electron field emission from carbon nanotubes by Ar neutral beam treatment. *Carbon* 2008;46(10):1316–21.
- [11] Kim JS, Ahn KS, Kim CO, Hong JP. Ultraviolet laser treatment of multiwall carbon nanotubes grown at low temperature. *Appl Phys Lett* 2003;82(10):1607–9.
- [12] Zhi CY, Bai XD, Wang EG. Enhanced field emission from carbon nanotubes by hydrogen plasma treatment. *Appl Phys Lett* 2002;81(9):1690–2.
- [13] Ahn KS, Kim JS, Kim CO, Hong JP. Non-reactive rf treatment of multiwall carbon nanotube with inert argon plasma for enhanced field emission. *Carbon* 2003;41(13):2481–5.
- [14] Weng CH, Leou KC, Wei HW, Juang ZY, Wei MT, Tung CH, et al. Structural transformation and field emission enhancement of carbon nanofibers by energetic argon plasma post-treatment. *Appl Phys Lett* 2004;85(20):4732–4.
- [15] Zhu YW, Cheong FC, Yu T, Xu XJ, Lim CT, Thong JTL, et al. Effects of CF<sub>4</sub> plasma on the field emission properties of aligned multi-wall carbon nanotube films. *Carbon* 2005;43(2):395–400.
- [16] Gohel A, Chin KC, Zhu YW, Sow CH, Wee ATS. Field emission properties of N<sub>2</sub> and Ar plasma-treated multi-wall carbon nanotubes. *Carbon* 2005;43(12):2530–5.
- [17] Feng T, Zhang JHH, Li Q, Wang X, Yu K, Zou SC. Effects of plasma treatment on microstructure and electron field emission properties of screen-printed carbon nanotube films. *Physica E* 2007;36(1):28–33.
- [18] Hou ZY, Cai BC, Liu H, Xu D. Ar, O<sub>2</sub>, CHF<sub>3</sub>, and SF<sub>6</sub> plasma treatments of screen-printed carbon nanotube films for electrode applications. *Carbon* 2008;46(3):405–13.
- [19] Lee K, Lim SC, Choi YC, Lee YH. Origin of enhanced field emission characteristics postplasma treatment of multiwalled carbon nanotube array. *Appl Phys Lett* 2008;93(6):063101.
- [20] Gui XC, Wei JQ, Wang KL, Xu EY, Lv RT, Zhu D, et al. Super-low turn-on and threshold electric fields of plasma-treated partly Fe-filled carbon nanotube films. *Mater Res Bull* 2010;45(5):568–71.
- [21] Kyung SJ, Park JB, Lee JH, Yeom GY. Improvement of field emission from screen-printed carbon nanotubes by He/(N<sub>2</sub>, Ar) atmospheric pressure plasma treatment. *J Appl Phys* 2006;100(12):124303.
- [22] Neupane S, Lastres M, Chiarella M, Li W, Su Q, Du G. Synthesis and field emission properties of vertically aligned carbon nanotube arrays on copper. *Carbon* 2012;50(7):2641–50.
- [23] Nilsson L, Groening O, Emmenegger C, Kuettel O, Schaller E, Schlapbach L, et al. Scanning field emission from patterned carbon nanotube films. *Appl Phys Lett* 2000;76(15):2071–3.
- [24] Dionne M, Coulombe S, Meunier JL. Screening effects between field-enhancing patterned carbon nanotubes: a numerical study. *IEEE Trans Electron Devices* 2008;55(6):1298–305.
- [25] Cui H, Zhou O, Stoner BR. Deposition of aligned bamboo-like carbon nanotubes via microwave plasma enhanced chemical vapor deposition. *J Appl Phys* 2000;88(10):6072–4.
- [26] Vincent P, Purcell ST, Journet C, Binh VT. Modelization of resistive heating of carbon nanotubes during field emission. *Phys Rev B* 2002;66(7):075406.
- [27] Dionne M, Coulombe S, Meunier JL. Energy exchange during electron emission from carbon nanotubes: considerations on tip cooling effect and destruction of the emitter. *Phys Rev B* 2009;80(8):085429–1–10.
- [28] Dionne M, Coulombe S, Meunier JL. Field emission calculations revisited with Murphy and Good theory: a new interpretation of the Fowler–Nordheim plot. *J Phys D Appl Phys* 2008;41(24):245304.
- [29] Coulombe S, Meunier J-L. Thermo-field emission: a comparative study. *J Phys D Appl Phys* 1997;30(5):776.
- [30] Nilsson L, Groening O, Groening P, Schlapbach L. Collective emission degradation behavior of carbon nanotube thin-film electron emitters. *Appl Phys Lett* 2001;79(7):1036–8.
- [31] de Jonge N, Bonard JM. Carbon nanotube electron sources and applications. *Phil Trans R Soc A* 2004;362(1823):2239–66.
- [32] de Jonge N, Allieux M, Doytcheva M, Kaiser M, Teo KBK, Lacerda RG, et al. Characterization of the field emission properties of individual thin carbon nanotubes. *Appl Phys Lett* 2004;85(9):1607–9.
- [33] Edgcombe CJ, Valdrè U. Microscopy and computational modelling to elucidate the enhancement factor for field electron emitters. *J Microsc* 2001;203:188–94.
- [34] Edgcombe CJ, Valdrè U. Experimental and computational study of field emission characteristics from amorphous carbon single nanotips grown by carbon contamination – I. Experiments and computation. *Philos Mag B* 2002;82(9):987–1007.
- [35] Kawabata A, Ota K, Matsuura T, Urayama M, Murakami H, Kita E. Improvement of field emission characteristics by fabricating aligned open-edged particle-free carbon nanotubes. *Jpn J Appl Phys* 2002;41(12A):L1363–5.
- [36] Bhattacharyya S, Cardinaud C, Turban G. Spectroscopic determination of the structure of amorphous nitrogenated carbon films. *J Appl Phys* 1998;83(8):4491–500.
- [37] Ma H, Berthier Y, Marcus P. NH<sub>3</sub> probing of the surface acidity of passive films on chromium. *Corros Sci* 2002;44(1):171–8.
- [38] Agouram S, Bodart F, Terwagne G. LEEIXS and XPS studies of reactive unbalanced magnetron sputtered chromium oxynitride thin films with air. *J Electron Spectrosc Relat Phenom* 2004;134(2–3):173–81.
- [39] Che RC, Peng LM, Wang MS. Electron side-emission from corrugated CN<sub>x</sub> nanotubes. *Appl Phys Lett* 2004;85(20):4753–5.
- [40] Doytcheva M, Kaiser M, Verheijen MA, Reyes-Reyes M, Terrones M, de Jonge N. Electron emission from individual nitrogen-doped multi-walled carbon nanotubes. *Chem Phys Lett* 2004;396(1–3):126–30.